A Virtual Prototyping Toolkit for Assessment of Child Restraint System (CRS) Safety

K.F. Hulme, A. Patra, N. Vusirikala
University at Buffalo

R.A. Galganski, I. Hatziprokopiou
General Dynamics Advanced Information Engineering Services

ABSTRACT

Computational modeling continues to play an increasingly significant role in the design of more effective vehicle crash safety systems. Models configured with sophisticated computer analyses permit researchers to perform extensive "what-if?" exploratory studies at a fraction of the cost and time that would be required by physical testing alone. Presently, our research team is developing a modeling and analysis capability that will provide child restraint system (CRS) engineers, designers, and analysts a validation tool that will supplement conventional engineering results attained from sled testing, which is often timely and costly. Supplementing these physical tests and digital modeling capabilities is the newly developed NYSCEDII CRS Visualization Module (NCVM), which allows a user to immersively visualize the MADYMO-calculated automotive crash simulation imagery. Depicted are the motion of, and interactions between, the CRS shell, human "dummy", harness and latch belt assemblies, and applicable vehicle cabin-interior surfaces and structure; and nodal finite element Von Mises color stress contours for the CRS shell and its attendant restraint straps. Supplemental NCVM features include: plotted instantaneous body segment acceleration-time responses; dummy displacements visually tracked using on-screen reference markers - to be tracked as a function of time; forwards or backwards animation capability; and stereo viewing, using anaglyphic stereo, to convey a sense of depth and immersion.

This paper demonstrates the utility of the NCVM using a combination conventional/finite element system model of a recent-production child restraint system (CRS) and its three-year-old dummy occupant in a modified FMVSS 213 sled test environment.

INTRODUCTION

In various parts of the world, child passengers riding in motor vehicles are subject to occupant injury criteria such as those embodied in U.S. Federal Motor Vehicle Safety Standard (FMVSS) 213 [1]. These regulations require that children within specified age and weight categories be constrained within a specially designed device, a child restraint system (CRS), which in turn is secured to the interior of the vehicle cabin. In each case, a rigorous laboratory test procedure (in the U.S., [2]) must be followed to ascertain CRS compliance relative to the stipulated safety requirements.

Currently, CRS prototype development and existing-design optimization are carried out almost exclusively via sled testing. Tooling and other costs associated with this often seemingly endless cycle - fabrication, testing, debugging, redesign, and fabrication - can mount rapidly, especially if too many educated guesses don't pan out along the way. These costs can be reduced, often substantially, by conducting a series of extensive "what-if?" exploratory studies at critical stages of the initial design and/or redesign process using a suitable analytical tool and supporting software. MADYMO (MAthematical DYnamical MOdels) [3], a state-of-the-art general-purpose analytical software package used extensively in the U.S. and abroad, was selected for this purpose in the research outlined below.

Our research team recently demonstrated that MADYMO analyses can be enhanced by providing users the sensation of immersion in a virtual crash environment. This capability is achieved by way of a newly developed post-processing utility called NCVM (NYSCEDII CRS Visualization Module), described in this paper. It is applied to a conventional/finite element system model of a recent-production CRS and its dummy occupant in a modified FMVSS 213 sled test environment.

The breakdown of the paper is as follows. First, a pertinent literature survey is presented. Next, technical details of the physical sled test will be outlined. This will be followed by a discussion of the MADYMO computer model that was generated to computationally simulate the test. This will then be followed by a detailed discussion of the design and development of the NCVM. Simulation results will be presented and discussed, after which some appropriate conclusions will be drawn. This paper

concludes with numerous suggestions for future avenues of research.

LITERATURE REVIEW

Child Restraint System (CRS) safety and design has been the focus of a fair amount of published research over the last 25 years. A brief survey of the literature demonstrates a wide-variety of past and present research efforts pertaining to CRS design, analysis, modeling, and safety assessment – all relevant concerns and motivating factors for the research at hand. Here, the authors have decomposed the present literature survey into 4 related subcategories:

a) CRS harness and seat design,
b) Forward vs. rearward facing child seats and misuse studies,
c) CAD, Modeling, and Simulation (CRS and child dummy),
d) CRS software utilities, commercial software, and dedicated CRS research projects.

a) *Tantamount to this research effort is related research pertaining to the design of both the child seat and accompanying harness belts – the CRS system itself.* An early study of vehicular CRS design traits by Trinca and Arnberg [4] demonstrated a number of important factors influencing the choice and practical utility of a child seat. These included: how easily the seat can be transferred from one car to another, how well the seat supports a very young child, the size, softness and degree of incline of the seat, how much space it occupies in the car, how easily the harness/buckle system are to use, and other factors. A more recent study [5] was conducted to assess usability issues relating to CRS harness design. Four convertible child restraint systems representing a variety of design features were used. The benefits and costs of these features were discussed, and a method to test harness design usability was presented. Certain design features were perceived by users as providing significantly better protection in the event of a collision, however, these also tended to be the features that were *misused* the most often. Another research effort by Lefeuve et al. [6] deals with the use of numerical methods in the design of a CRS. Specifically, a numerical simulation of the CRS was performed using both an elasto-static model and an elasto-dynamic approach.

b) When designing software models that attempt to emulate a CRS arrangement, one must take into consideration usage procedures, both proper and incorrect. The primary objective of a study by Arbogast et al. [7] was to determine the effectiveness of forward facing child restraint systems (FFCRS) in preventing serious injury and hospitalization as compared with similar age children restrained solely in seat belts. As compared with seat belts, CRS were found to be highly effective in preventing serious injuries and hospitalization, respectively. The effectiveness estimate attained was found to be substantially higher than that determined from older estimates, demonstrating the benefits of *current* CRS designs. Another research effort by Carlsson and Ysander [8] pointed out that the major emphasis of recent CRS studies is placed on the benefits of using rearward-facing child seats for children 0 to 4 years of age. Attitudes concerning child safety in cars and the misuse problem were also discussed, and based on Volvo's accident material, it is shown that the injury-reducing effect of the rearward-facing child seat is superior to all present types of child restraints in cars. In another related research paper by Czernakowski and Müller [9], a quantitative method of predicting and assessing misuse of CRS is proposed. The process, called "Misuse Mode and Effects Analysis (MMEA)", assesses the likelihood of occurrence of potential misuse modes and their effect on safety before and after corrective actions. The effectiveness of the proposed method was demonstrated in the assessment of a number of commonly used CRS devices.

c) *Numerous more recent research efforts have attempted to model and analyze the structural behavior of past and present CRS (and human model) designs.* A recent study by Noureddine et al. [10] saw the development of a finite element model of the Hybrid III crash test dummy for computer crash simulations. A description of the major components of the Hybrid III dummy and their finite element representations were supplied. The reasonable accuracy obtained from the model makes it useful for crashworthiness simulations when combined with other vehicle and restraint system models. Another more generic study by Arlt and Marach [11] saw the enhancement of the pre-existing program "RAMSIS" (a CAD-tool for ergonomic analysis of vehicles developed for the German automotive industry). This computer aided resource made it possible to create a real geometric and kinematic model of the human body. Up until recently, the different RAMSIS body types were adults, so it was not possible to make statements on the quality of a car interior from the point of view of *children*. Hence, for this research, it was necessary to develop a realistic 3-D child model that could be used by the designers for seat and safety analysis on a CAD-system. Concerning vehicular modeling, a recent study by Thacker et al. [12] saw the development of a finite element automobile model for use in crash safety studies, which was developed through reverse engineering. The model was designed for calculating the response of the automobile structure during full frontal, offset frontal, or side impact collisions. The reverse engineering process involved the digitization of component surfaces as the vehicle is dismantled, the meshing and reassembly of these components into a complete finite element model, and the measurement of stiffness properties for structural materials. Yet another very recent (and relevant) published research effort by Klinich et al. [13] saw a combination of finite element modeling and sled test reconstruction of real-world head injury scenarios to investigate infant head impact response and tolerance to skull fracture. A finite element model of a six-month-old infant head was also developed using available material properties and "human-like" geometry. The infant head FEM was used to simulate different injury and no-injury loading conditions based on CRS response data from the reconstruction tests.

d) *Finally, our survey of literature showed the presence of numerous softwares and large-scale funded research efforts dedicated to CRS design and development.* The funded CREST project [14] ran for 4 years and was completed at the end of 2000. The project's aim was to gain better understanding of the way child restraint systems behave in crashes by investigating real world accidents and conducting full-scale reconstructions of a selection of those crashes. The Vehicle Safety Research Centre's (VSRC) contribution to the project involved crash investigation, correlating medical data and obtaining detailed data from vehicle examinations, police information and the restraint systems. Virtual testing has grown to be an efficient tool in vehicle design and allows the integrated evaluation of various design aspects, thereby reducing prototyping costs and time to market. Virtual testing also provides an efficient extension of existing standardized tests to real-life crash conditions. ADVISER (developed by ADVANCE and VITES in Europe, and now owned by TNO-Automotive) [15] automatically correlates numerical and experimental data and provides a corresponding quality rating for a numerical model. Stochastic simulations performed and analyzed with ADVISER provide insight in the sources of scatter in regulated crash tests and the effects this has on, for example, the injury criteria measured in model dummies. Yet another highly relevant and more recent European research project is Advanced Protective Systems (APROSYS) [16], which will focus on scientific and technology development in the field of passive safety (crash safety). The field of passive safety concerns in particular: human biomechanics (injury mechanisms and criteria), vehicle and infrastructure crashworthiness, and occupant and road user protection systems. The general objective of APROSYS is the development and introduction of critical technologies that improve passive safety for all European road users in all relevant accident types and accident severities. Sub-objectives include improved mathematical models of CRS arrangements and human dummies, and enhanced virtual testing for crash protection methods.

The present research endeavor involves numerous participants from a variety of research, academic, and industrial entities, namely: General Dynamics Advanced Information Engineering Services, the Center for Transportation Injury Research (CenTIR), Calspan-University at Buffalo Research Center (CUBRC), Applied Computational Mathematics and Mechanics Research Group (ACM^2E), and the New York State Center for Engineering Design and Industrial Innovation (NYSCEDII) at the University at Buffalo. It involves three focus areas pertaining to CRS safety and design. **Each of these focus areas - as evidenced by the above literature review - have been addressed separately, but never combined and integrated to the extent proposed here.** They are: i) physical sled testing, ii) digital computer modeling and finite element analysis, and iii) scientific immersive visualization. In our collaborative research efforts, we are first performing physical sled tests to attain reliable, standardized "conventional" engineering crash test data. The physical testing phase is followed by modeling, simulation, and analysis of the CRS/dummy arrangement in the hopes of validating our computer model relative to the physical tests. As sled testing can be both timely and costly, our research group is striving to attain a digital modeling capability that will allow us to supplement this experimental approach. Finally, we are incorporating the use of state-of-the-art 3-D-immersive visualization as a means of understanding, interpreting, and revising our results, which will allow for the continual improvement and refinement of our computer models. Our sled testing protocols are discussed in the next section; the modeling, analysis, and visualization research will be discussed in later sections.

SLED TESTING

The MADYMO model (fully described in the next section) was "validated" in a series of sled test experiments performed at General Dynamics' HYGE sled facility. A current-production 5-point harness child restraint system (CRS) accommodating a Hybrid III 3-year-old child dummy was positioned upright on a modified FMVSS 213 test bench (described below) in the forward-facing installation mode. It was equipped with the standard array of electronic instrumentation: head- and upper torso-mounted triaxial accelerometer packages, upper neck force- and moment-measuring transducers, and a transducer that records chest compression.

Two series of three replicate tests, involving two slightly different conditions, were conducted with the same CRS (i.e., a total of six tests were performed). The first series (test nos. 11-3-01, 11-3-02, and 11-3-03) utilized the tether strap; the second set (test nos. 11-3-04, 11-3-05, and 11-3-06) did not. Figure 1 depicts two views of a typical pre-test setup.

Figure 1a: Pre-test – North side of CRS

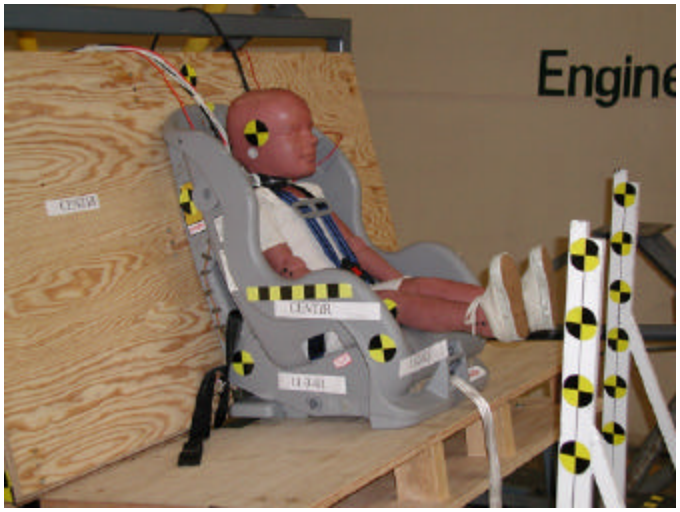

Figure 1b: Pre-test - South side of CRS

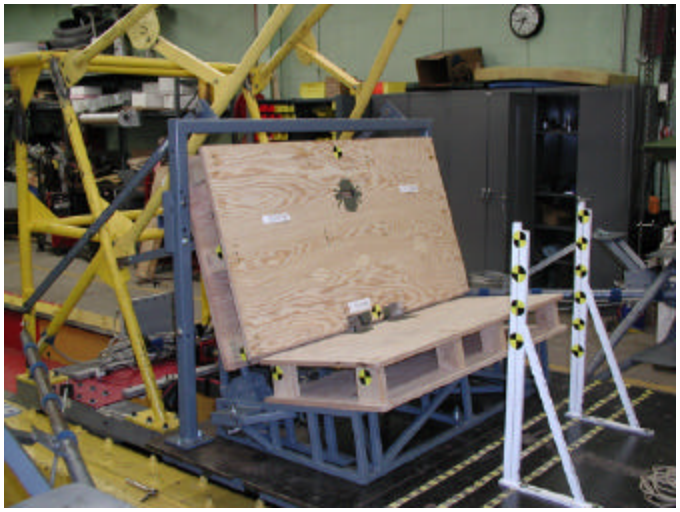

Figure 2a: Hard test bench (front view)

Several changes were made to the FMVSS 213 test procedure in an effort to simplify the model and thus increase the possibility that its predictions would more closely match those obtained experimentally. The most notable of these was predicated on (1) the inherent complexity of the dynamic interaction between the CRS, dummy, and the bench upon which the base of the CRS rests; and (2) the absence of critical test bench material property inputs utilized by the MADYMO code. As such, the standard test bench, which consists of a "soft" seat cushion and seat back,[1] was replaced. Instead, "hard" assemblies, having the same overall exterior dimensions and geometry as their original counterparts, were used. The latter units were constructed from ¾-inch-thick plywood and short lengths of nominal standard 2 x 4 (inch) lumber. Figures 2a and 2b show the modified test bench bolted in place to the existing steel framework.

[1] The FMVSS 213 test bench seat cushion and seat back assemblies feature a laminated construction: two slabs of polyurethane foam having different density and thickness, the stiffer of which is in contact with a 3/8-inch-thick sheet of plywood. This "sandwich" is encased in a tight-fitting jacket made from elastic-backed vinyl automotive upholstery, circa early 1970s.

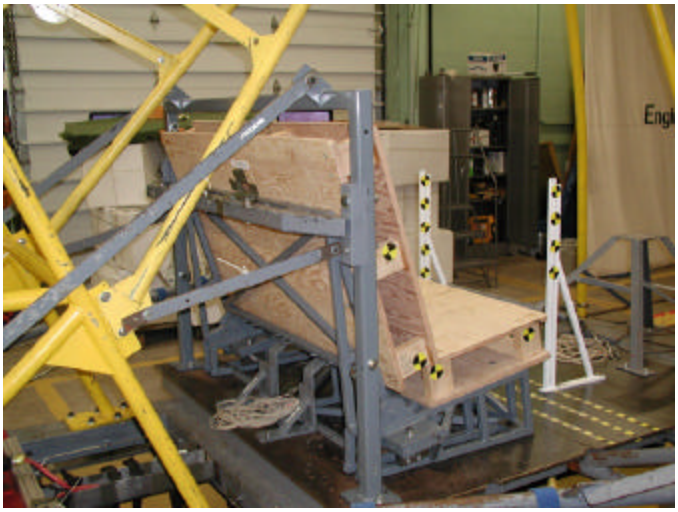

Figure 2b: Hard test bench (rear view)

In another attempt to improve the fidelity of the computer simulation, the seat back portion of the modified test bench was constrained against pitching action to eliminate possible inertial loading of the CRS during the tethered-configuration tests.[2] This objective was met by bolting two steel bars - one per side - between a vertical seat back frame member and the sled carriage structure.

Figure 3: Latch belt used to secure the CRS to the sled carriage

The CRS was secured to the sled carriage by a manufacturer-supplied seat belt assembly - commonly referred to as the "latch belt" - which passes through the appropriate belt path in the CRS shell. Each end snapped onto a belt anchor located below and behind the top plywood surface of the test bench seat "cushion". The free end of the webbing was then pulled through the buckle assembly until the belt could not be tightened any further. Figure 3 presents a side view of a latch belt in place just prior to a typical test. The above-noted anchors are shown in Figures 4a (the two arrows indicate their exact location relative to the longitudinal centerline of the test bench) and Figure 4b (a close-up side view).

[2] Conventional FMVSS 213 testing permits the soft seat back and its supporting framework to rotate about its pivot point.

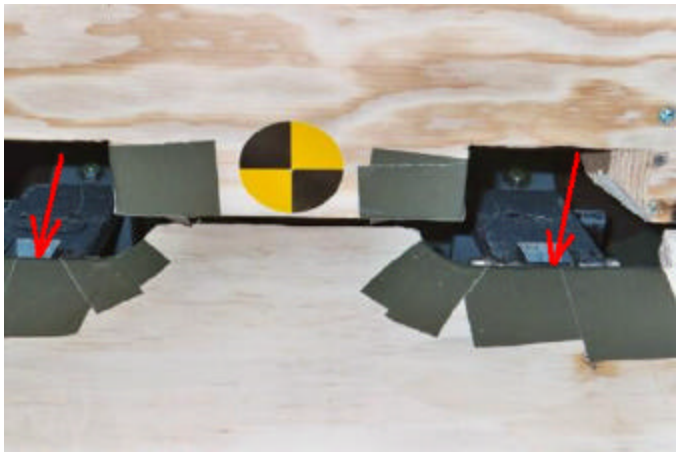

Figure 4a: Latch belt anchors

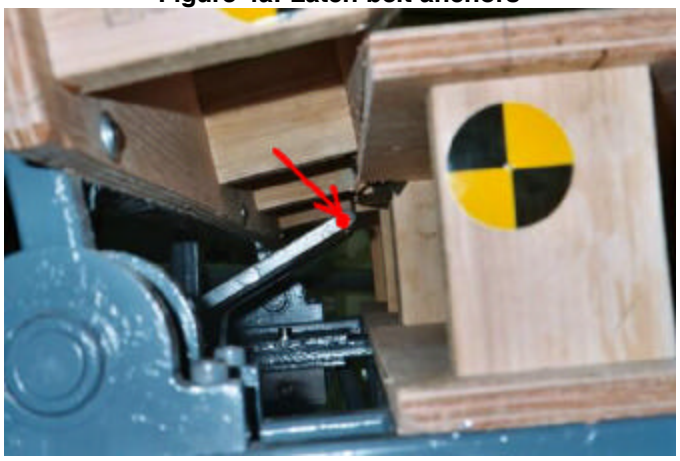

Figure 4b: Latch belt anchor (side view)

Other noteworthy departures from the FMVSS 213 test protocol included:

- Removed the foam/fabric cover on the CRS plastic shell.
- Installed load cells to record the tensile force variation in the upper torso harness straps and the tether strap.
- Deployed three (instead of the customary two) high-speed video cameras:

    1) a side-mounted narrow field-of-view camera to record CRS and dummy excursions consistent with the compliance test procedure.
    2) a side-mounted wide field-of-view camera to capture the entire interaction between the CRS, dummy, and the test bench seat back surface during the rebound phase of the action.
    3) a front-mounted camera along the longitudinal centerline of the sled carriage to record frontal-perspective CRS and dummy kinematics.

In addition, several strain gage rosettes recorded strains at anticipated high-stress locations on the CRS shell. The data is currently being processed and may be presented as part of a planned future paper.

Figure 5 presents a front view of the CRS with the dummy installed in a typical pre-test setup. Both upper straps comprising the harness assembly (which secures the dummy to the safety device) were threaded through their respective top-level slots in the shell, with the above-noted load cells installed near the dummy's shoulders. Prior to each test, the harness was hand tensioned as tight as possible and the chest clip adjusted to the same location relative to the harness buckle and latch plate assembly.

Figure 5: CRS Front view (w/ dummy)

Figure 6: Tether mounting location on the CRS shell

Photos showing a typical tether strap configuration employed in the final three tests are presented in Figures 6 through 9. The arrow in Figure 6 points toward the origin of this belt - a thick double-slotted metal plate (designed to accommodate a loop in the fabric) lying flush against the rear shell wall, approximately 16.5 inches above the CRS base. There, the tether passed through a notch (indicated by the arrow in Figure 7) in the front-facing plywood panel of the test bench seat back, emerged through an identical notch on the rear panel of the seat back, and was clipped to an anchor mounted on the sled carriage framework, where it was hand tensioned to the maximum degree possible (see Figure 8). The load cell (denoted by the arrow in Figure 9) was installed on the webbing spanning the gap between the two panels.

Figure 7: Front side of test bench seat showing location of notch made for tether

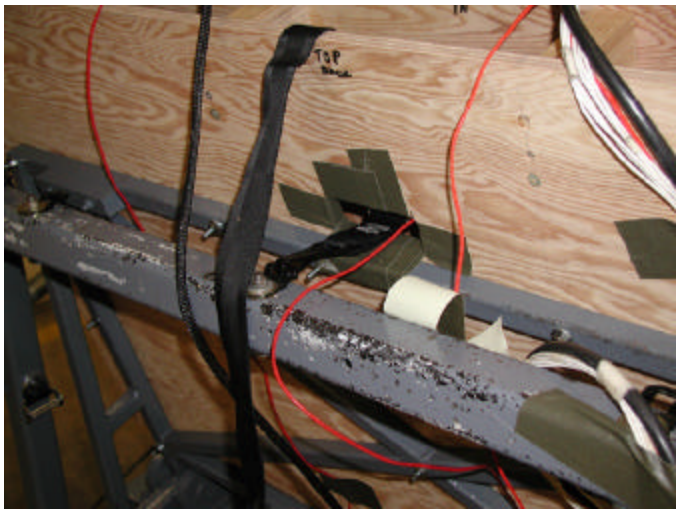

Figure 8: Tether anchorage behind the test bench

Each test produced virtually identical acceleration pulses within the corridor stipulated by FMVSS 213. The average sled carriage velocity change was 29.7 mph. Figure 10 depicts a typical sled acceleration pulse.

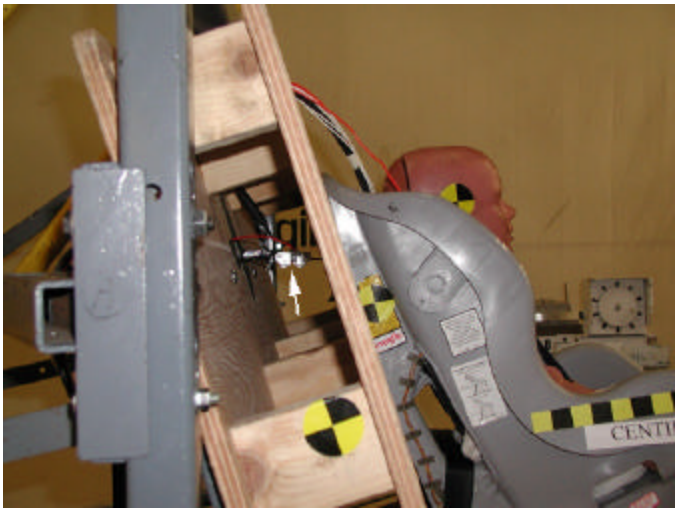

Figure 9: Tether load cell

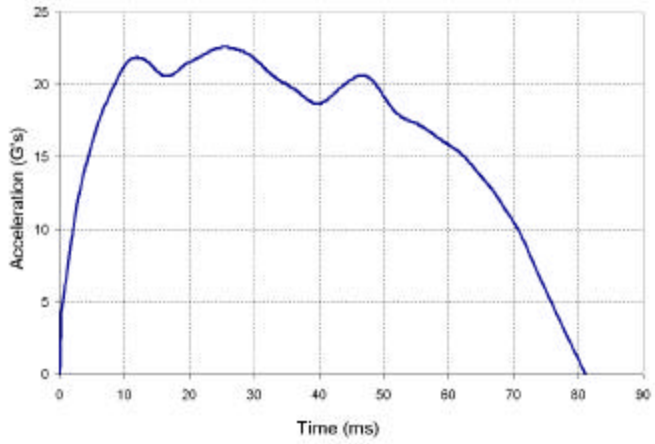

Figure 10: Typical sled acceleration pulse

Figure 11 presents two photos showing the CRS and dummy following a typical test. The CRS incurred no visible damage during the first three (with-tether) tests. Peak harness and tether belt forces were well below their respective maximum design elastic limit, confirming the observed absence of any permanent belt stretch after each test.

The fourth test - the first without the tether (no. 11-3-04) - produced the first visually apparent damage to the CRS. Two small cracks formed in the upper portion of the shell (indicated by the arrows in Figure 12). The south-side wide field-of-view camera clearly revealed the causal mechanism: head contact with the region during rebound-induced CRS impact with the test bench seat back. Figure 12 shows that the cracks were in relatively narrow strips of plastic in an area containing several slots. As such, it was not regarded as a *structural* failure per se, thus justifying continued testing. Inspections following the two remaining exposures showed that neither one exacerbated the existing cracks nor caused additional shell damage elsewhere. Harness belt loadings were once again well within the elastic range for all three tethered-condition tests.

Figure 11a: CRS and dummy appearance immediately after a typical sled test (North)

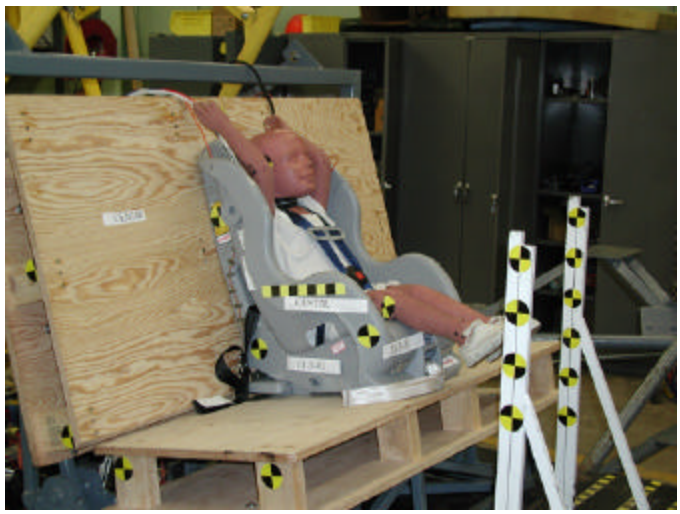

Figure 11b: CRS and dummy appearance immediately after a typical sled test (South)

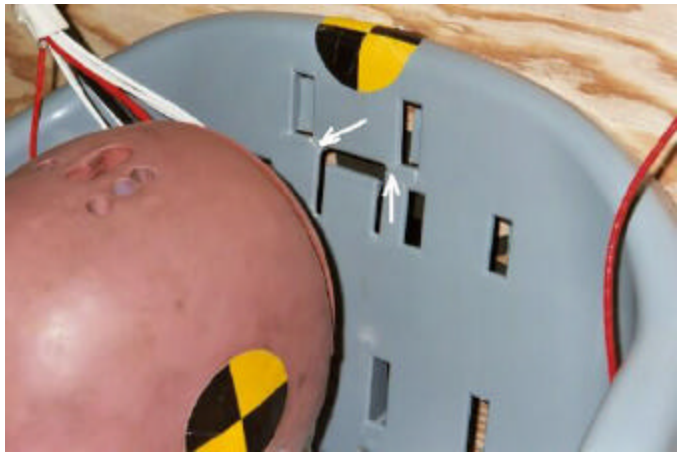

Figure 12: Small non-structural cracks in the CRS shell detected after test 11-3-04

Finally, values of FMVSS 213 occupant injury-indicating parameters and other measurements obtained from the test program are summarized in Tables 1 and 2, both found in the Appendix.

The next section details how the MADYMO model was constructed to provide a reasonable approximation to the videotaped dummy kinematics and the physical quantities tabulated in the above-noted tables.

MODEL AND SIMULATION DESCRIPTION

The MADYMO model created for use in this study is intended to mimic the salient parts of the various systems and subsystems comprising the modified FMVSS 213 sled test setup described in the previous section. As such, it includes relatively simple idealized representations of the CRS (including its harness belt assembly), a standard Hybrid III dummy [17] located and restrained within the confines of the CRS, the test bench assembly on which the CRS was placed and positioned, and the safety belt that secures the CRS to the sled carriage structure.

Material compliance properties (i.e., force-deflection and energy absorbing characteristics) and several other material-related parameters utilized by MADYMO were generally unavailable, requiring the use of assumed or best-estimate values gleaned from various sources. The planned follow-on to this project will endeavor to improve the accuracy of all such inputs.

The CRS shell, whose thickness is considerably less than its characteristic curved- or flat-plane dimensions, is appropriately configured using shell-type finite elements (FE). These elements, which are also more computationally efficient than their 3-D solid counterparts, were meshed using Hypermesh v5.0 [18]. The initial model idealized the interaction between the CRS base and the test bench seat "cushion" as a surface-to-line contact, an unrealistic assumption. It was consequently upgraded to reflect a surface-to-surface contact, consistent with the actual test setup (see Figure 13).

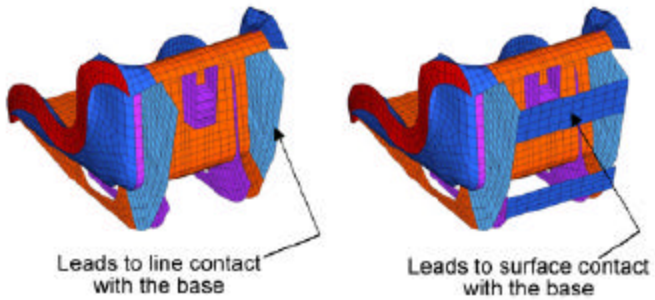

Figure 13: Bottom view of CRS shell FE model without base (left) and with base (right)

The wooden "cushion" and foam-filled back portions of the sled carriage test bench were both initially modeled as two rigid planes connected to inertial space. The (primarily) sliding contact that occurs between the bottom of the CRS and the cushion did not adversely affect the simulation to any significant degree. Rebound-induced impact between the CRS back surface and the front surface of the test bench back, however, did. Accordingly, the latter interaction was subsequently modeled as an *inelastic* contact. This representation in

turn was replaced by an elastic contact interaction when actual foam material compliance data [19] were finally obtained.

The individual belts comprising the harness assembly are all idealized as hybrid models consisting of a FE belt model connected to a conventional belt model [3] at each end.[3] The latter elements provide the mechanism to prescribe FE belt tension and are instrumental in studying the effects of belt slack. Figure 14 (found in the Appendix, due to its size) depicts the complete MADYMO computer model employed in this study.

In an actual HYGE sled test, a prescribed x- or longitudinal-direction acceleration pulse (see, e.g., Figure 10) is applied directly to the sled carriage. The carriage and an attached simulated cabin or test fixture move backward, causing an initially at-rest occupant "connected" in some manner to one of those systems to *move forward relative to the cabin or fixture*. The so-called sled pulse can thus be applied directly to the dummy as a fictitious acceleration field and the calculated accelerations corrected to obtain the "correct" values. This process eliminates the need to model the sled carriage itself.

Acceleration inputs to the model employed in this study consisted of the abovementioned sled pulse data and the constant downward-acting (i.e., in the z-direction) gravity field. The total simulation run time was prescribed as 200 milliseconds, more than enough time to observe the effects of CRS interaction with the test bench seat back during rebound.

Selected MADYMO-generated animation-file (kn3) data provided by the model depicted in Figure 14 will be utilized in the next section to illustrate some of the features incorporated in the newly developed immersive visualization tool for assessment of CRS safety - the NCVM.

THE NYSCEDII CRS VISUALIZATION MODULE (NCVM)

INTRODUCTION AND PREPROCESSING

The NCVM incorporates all of the geometric and structural information from a TNO-MADYMO simulation into a single, all-encompassing scientific visualization. The visualization has been written in OpenGL [20], which allows for usage on multiple platforms, including PC, and SGI/Sun workstations. The NCVM is highly menu-driven, and allows for a variety of user-interactive features. The fully-integrated functionality of the NCVM will provide a new mechanism by which scientists and engineers can more quickly and easily make design decisions pertaining to a CRS simulation. The NCVM initializes by parsing and pre-processing the pertinent TNO-MADYMO output files, including geometry (.kn3), stress (.fai), and acceleration (.lac) details over a 0.2 second time interval for a non-destructive "reverse" crash test simulation. Once the data is parsed and arranged within appropriate arrays, the geometry is generated and drawn for the initial (i.e. time = 0.0) time step. For each frame of the simulation (of which there are 67 in full, each representing 0.003 second time intervals), all graphical entities (i.e. the human, the seat, the seat belt straps, the car, etc.) have been modularized in separate functions, and cached and stored in OpenGL *Vertex Arrays*, to optimize the graphical performance of each animation frame. Vertex Arrays will be described contextually in greater detail in Part II of this section of the paper.

GEOMETRIC REPRESENTATION

To generate the geometry from the MADYMO .kn3 file at each time step, simple OpenGL primitives are utilized, and described as follows. Because there are *thousands* of nodes in the seat and seat belt/lap belt strap finite element models, it is necessary to use solid primitives with as few vertices as possible – hence the choice of the cube primitive, which has 8 corner vertices. The "frame" structure behind the child seat has been modeled using 2 simple planar quadrilaterals, and the seat springs (which affix the child seat to the rigid frame) have been modeled using line segments. The generation of the human geometry requires the use of hyper-ellipsoids, for which a new OpenGL primitive class has been created (coined a "gluEllipse", which is a modified version of the pre-existing OpenGL "gluSphere" routine). Baseline kn3 geometries, as just described, are seen in Figure 15.

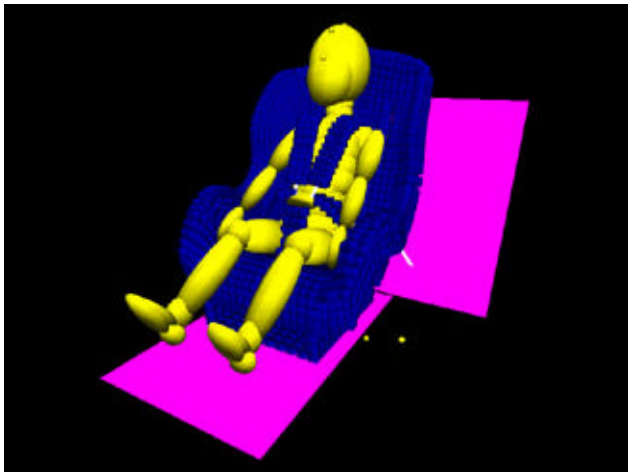

Figure 15: Baseline CRS geometry

To enhance the realism of the visual simulation, and to add context for the crash simulation, numerous (non-kn3) geometric entities have been added to the field of view. These include a model vehicle in whose back seat the physical child seat resides, and a simple representation of a "crash wall". The simulation begins with a simple forward driving motion leading up to the moment of impact, whereupon the crash simulation of interest begins. The baseline geometry is shown with these graphical enhancements in Figure 16.

[3] MADYMO's conventional belt is a massless, uniaxial element that does not exhibit bending or torsional stiffness. In a systems context, it can be thought of as a spring connected in parallel to a damper. Spring and damper forces are calculated at the belt attachment points.

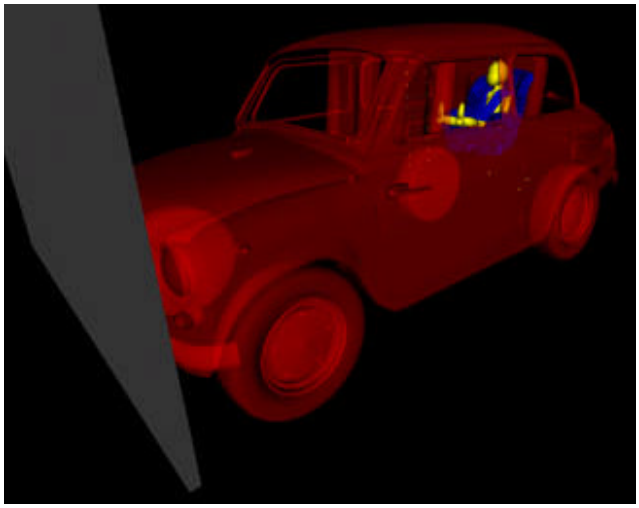

Figure 16: Enhanced CRS geometry

To allow for faster performance or greater detail, the user can interactively alter the level-of-detail of the graphical details of the visualization for lower/higher fidelity, as appropriate. For example, to allow the user to visualize certain stress "hot spots" in the model that might be obstructed by other elements of the simulation, the user can toggle on/off any graphical details of the simulation (i.e. the human model, the seat model, the belt strap models, etc.) at any time. A top-view close-up is shown in the following Figures 17 and 18 - the first with, and the latter without, the human model shown.

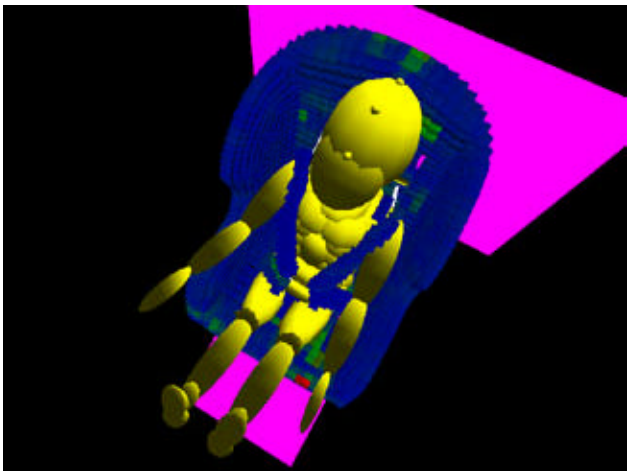

Figure 17: Top-view with human visible

SCIENTIFIC VISUALIZATION –
FINITE ELEMENT AND ACCELERATION DATA

The ability to visualize geometric displacement at every time step is only one aspect of the NCVM. For the visualization to be truly scientific in nature, useful technical data has been incorporated into the visual simulation to coincide with the motion of the child seat and the human torso (geometric) models. The first class of such information is stress data. The .fai MADYMO output file yields Von Mises stress data at each element in each of the finite element models (i.e. the seat, the lower left and right belt straps, and the upper left and right shoulder straps). Recall that our geometry for the seat and belt shoulder straps are displayed at the finite element *nodes*. One of the datasets that is parsed in the .kn3 file is data that dictates which nodes belong to each finite *element*. A "reverse sorting" procedure is thus performed to determine which finite elements belong to each node. With this information, one can then perform a simple linear interpolation to closely approximate the stress levels at each finite element node. This allows us to color-code each geometric node with stress contours at each and every time step. Also provided is an on-screen textual description of max/min/mean stress at each time step.

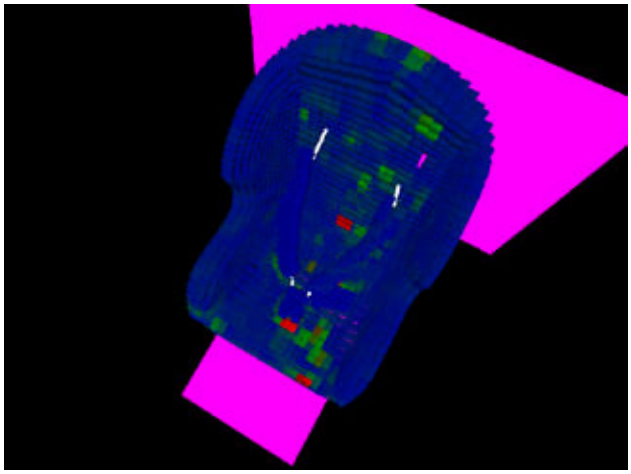

Figure 18: Top-view with human invisible

The user can alter the scale of the stress data dynamically. There are three possible stress scales: absolute (which uses the overall min and the overall max over the entire duration of the simulation), logarithmic (uses a natural log scale to compress the stress range to a smaller numerical region), or dynamic (absolute min/max stress data is used, but it changes each and every time step). Likewise, since there are 3 different types of finite element models (the child seat, the lower belt straps, and the shoulder straps), each of which are comprised of different materials and are likely to be subjected to different stress ranges, the user can toggle on/off visible stress ranges between the three models. Figure 19 depicts a screen shot with relevant finite element contour information shown.

Another potentially useful class of technical information is the NCVM's ability to track the acceleration (x, y, z, and resultant) of the human form during the crash simulation. The user can track acceleration of the human lower torso, upper torso, and head for every time step using an on-screen plotting utility. Color-coding is used to differentiate the three different acceleration entities – red, green, and blue, respectively. Again, a textual description of max/min/mean acceleration is provided for each and every time step. The default plotting mechanism is to show the graph interactively, along with the crash test motion, in the lower left portion of the screen. Should the user wish to see more intricate plotting details, one can switch to "full screen" plotting mode to observe the acceleration behavior at each individual iteration. Figure 20 depicts a screen shot with relevant resultant acceleration data plotted and maximum values listed for each of the three acceleration entities.

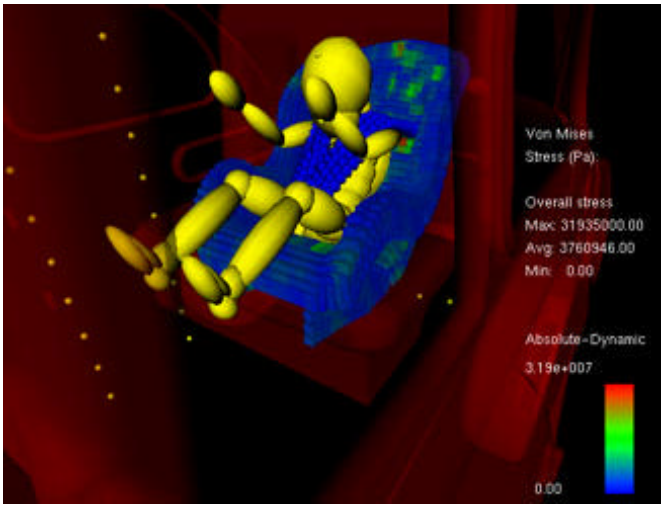

Figure 19: Finite element contour plotting

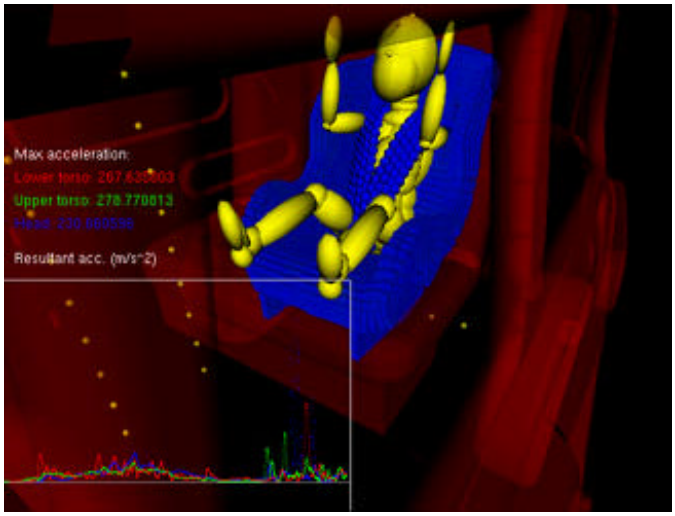

Figure 20: Acceleration plotting feature

OTHER VISUALIZATION OPTIONS

As previously explained, the child seat crash simulation has been placed within the context of a model vehicle. To better see the intricate details of the crash seat up close, the user may wish to de-emphasize the exterior automotive details by adjusting its transparency. The user can adjust the alpha blending values of the vehicle using the keyboard, such that it is somewhere between "fully-visible" (default) to "fully invisible", respectively.

To convey a sense of depth and immersion, the user can view the simulation in stereo. The visual simulation can be viewed in high-fidelity "active" stereo for expensive visualization display systems with auxiliary hardware (namely, a stereo emitter and high frequency shutter glasses). As a lower-cost alternative, the user can view the simulation in stereo, irrespective of hardware sophistication, using a low-fidelity 2-color anaglyphic stereo [21]. The user can view the simulation in the two most popular anaglyphic color pairs (Red-Blue or Red-Cyan) using an inexpensive pair of anaglyphic stereo glasses. The generation of stereo images on the screen clearly requires two distinct images in the left and right OpenGL buffers. The apparent distance between these images on the screen is dictated by what is commonly known as Interoccular distance, which is the distance between the left and right "eyes" of the viewer. This distance has a great deal to do with the success of the stereo effect, and the user can adjust this distance, up or down, using the keyboard. Figure 21 shows a close-up of the child seat, as does Figure 22, in a corresponding Red-Blue anaglyphic stereo screen capture.

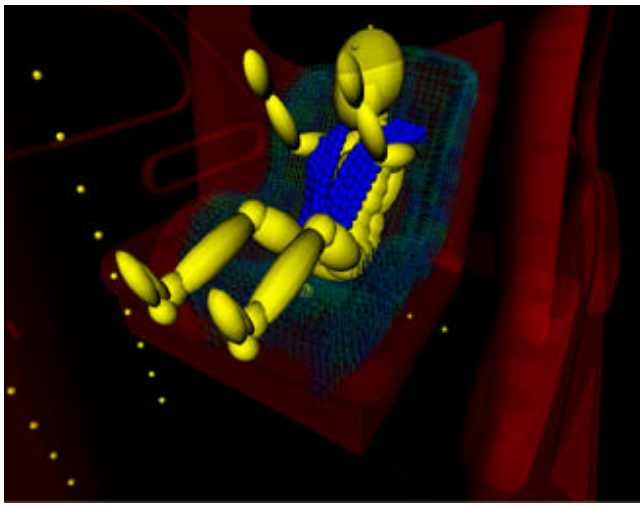

Figure 21: Full-color close up

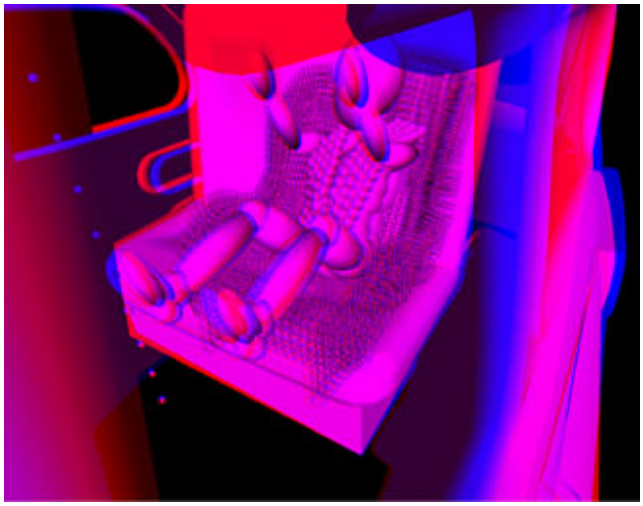

Figure 22: Anaglyphic stereo close-up

RESULTS AND DISCUSSION

This section compares corresponding computer-generated and experimental (i.e., sled test) results in an effort to evaluate the fidelity of the MADYMO composite model.

CHEST ACCELERATION ANALYSIS

Figure 23a (see Appendix) compares the dummy resultant chest acceleration recorded in the sled test *(non-tethered, 2nd case: 11-3-05)* to the same physical response generated by the MADYMO simulation over a duration of 200 milliseconds (ms). The maximum resultant acceleration is comparable in both simulation and experiment. In the first phase of the event (0 to 100 ms), we see a gradual rise and fall in acceleration with respect to time in the experiment, which is also predicted by the

simulation results. Our simulation shows an early peak between 15 and 30 ms, which is not seen in the experiment. We hypothesize that there is a time lag in the experimental observations - in the experiment, the input load is applied to the sled, whereas in the simulation, the load is applied to the dummy directly. Because the harness was pre-tensioned, there exists an inertial loading that was not modeled in the simulation. We can also notice that the width of the peak band (defined here as acceleration magnitudes in excess of about 25 G), is close to 50 ms for both curves. The modeling of the base of the seat is approximated for simplification because there are minor discrepancies in the kinematics of the seat and the way it comes into contact with the test bench. This was the reason for a sharp peak seen at 120 ms. The acceleration response between 140 and 200 ms primarily reflects the consequence of CRS contact with the test bench back during the protective device's rearward motion. Model-predicted acceleration magnitudes are almost equal to that of the corresponding experimental values. The modeled interaction may be more rigid than it actually is in the physical test, and hence the acceleration peak in the simulation occurs before the value is actually recorded in the experiment. Another factor, which influences the time at which the contact occurs, is the position and angle of the seat on the sled bench, which cannot be reproduced in the model exactly as they were in the experiment.

HEAD ACCELERATION ANALYSIS

Figure 23b (see Appendix) compares the dummy resultant head acceleration recorded in the sled test *(non-tethered, 2nd case: 11-3-05)* to the same physical response generated by the MADYMO simulation over duration of 200 milliseconds. Both the curves are fairly similar except for an early peak in acceleration in the simulation, as was the case with the previously described chest accelerations.

The maximum acceleration, in both experiment and simulation, is almost equal. In contrast to the fluctuations seen in Figure 23a for the chest simulation data, we see a smoother response for the head acceleration data. This is due to an elastic contact interaction between the seat and the dummy that was **not** modeled. This potential influence does not affect the head motion and hence the smooth observed response.

As an additional mechanism for model "validation", we have compared excursion values for head and knee. Here, "excursion" implies the relative forward displacement of the body. Both head and knee excursions are measured relative to the test bench pivot point. Table 3 shows the sled test/MADYMO comparison, which is very favorable.

Case	Head (in.)	Knee (in.)
Sled test (*11-3-05*)	21.2	23.9
MADYMO simulation	20.7	23.4

Table 3: Excursion Comparison

CRS MISUSE PARAMETRIC STUDY

This section presents a brief "what if?" study using the MADYMO CRS model to ascertain the effects of selected changes involving harness and/or latch belt tensioning on CRS performance. Table 4 lists the five cases considered. Case 1 provides MADYMO-predicted results *for properly tensioned belts*. Cases 2 and 3 examine the implications of two "incorrect" harness system tensioning levels while cases 4 and 5 do the same for similarly incorrect latch belt usage.

Case 1	Correct Use Simulation
Case 2	Harness - 14.3 % loose
Case 3	Harness- 33.4 % loose
Case 4	Latch belt - 15.0 % loose
Case 5	Latch belt - 30.0 % loose

Table 4: Test case details

Peak chest and head resultant accelerations for different test scenarios are compared in Figure 24 for the conditions described in Table 4. Knee and head excursions obtained for different test cases are compared in Figure 25.

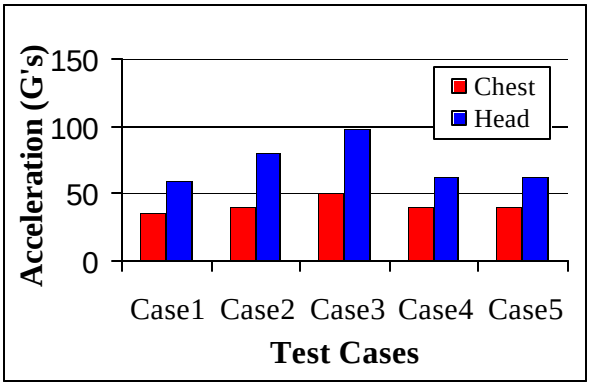

Figure 24: Chest/head - peak acceleration

Examination of these charts in conjunction with the chest acceleration plot depicted in Figure 26 (see Appendix) leads to the following CRS-misuse observations. Note that these observations are relative to the MADYMO-model forecasted (i.e. "Case 1") baseline:

- A loose harness produces a corresponding large rise in peak chest and head acceleration levels. Conversely, slack in the latch belt has a relatively minor effect on peak accelerations.
- Knee and head excursions increase moderately with increasing latch belt slack.
- Loose harness conditions produce a slight to moderate rise in head translation accompanied by a very small decrease in knee displacement.
- A loose harness causes higher peak chest accelerations later in the event.

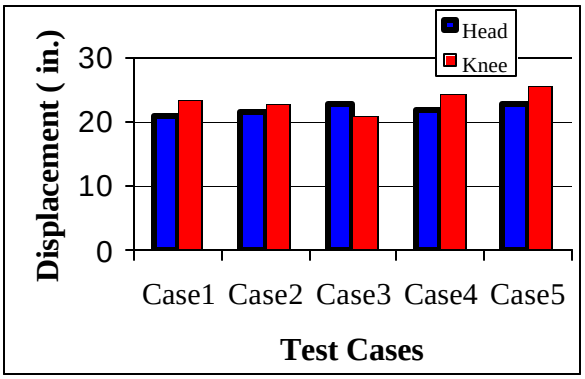

Figure 25: Knee/head - excursions

Analysis of the results provided by a more extensive series of CRS-misuse conditions revealed that the translation (and accompanying pitching action) experienced by the dummy at 38% belt slack leads to head contact with the seat cushion, producing an undesired high head acceleration response.

CONCLUSIONS AND FUTURE WORK

The research presented in this paper involves three primary focus areas pertaining to CRS safety and design. Each of these focus areas have surely been addressed in past literature and research, but never combined and integrated to the extent proposed here. These focus areas are: *i) physical sled testing, ii) digital computer modeling and finite element analysis, and iii) scientific immersive visualization*. In our collaborative research efforts, we first perform physical sled tests to attain reliable, standardized "conventional" engineering crash test data. The physical testing phase is followed by modeling, simulation, and analysis of the CRS/dummy arrangement, in the hopes of validating our computer model to the physical tests. The current model displays "good" correlation between those experimental and model-predicted physical parameters that can be (at least from an approximate standpoint) directly compared - specifically, maximum-allowable dummy head, chest, and knee responses stipulated by FMVSS 213.

Our research group is striving to attain a digital modeling and scientific visualization capability that will allow us to supplement or otherwise augment our physical sled testing procedures. To this end, we are incorporating the use of state-of-the-art 3-D, immersive visualization as a means of understanding, interpreting, and revising our results, which will allow for the continual improvement and refinement of our computer models. This visualization utility, the NCVM, is an OpenGL-based simulation that incorporates all of the geometric and structural information from a TNO-MADYMO simulation into a single, all-encompassing scientific visualization. This fully-integrated functionality of the NCVM will provide a new mechanism by which scientists and engineers can more quickly and easily make design decisions pertaining to a CRS simulation, as demonstrated in the case study found in this paper.

Our work to date integrating experiments, finite element/kinematics analysis and visual post processing has set the stage for some very exciting ongoing studies and development. We conclude this paper by listing these:

USE OF CURRENT MODELS

- Exercise current model with crash pulse from NCAP 35 mph flat frontal barrier crash test. Compare predicted CRS performance to that forecasted for FMVSS 213 test conditions.
- Perform additional perturbation studies with the small-mesh model to examine the effects of alternative vehicle (sled) CRS-securement seat belt anchorage locations, sled test bench geometry, sled test bench foam material compliance properties, and frontal crash sled pulses.
- Develop a MADYMO model that simulates CRS performance in typical off-standard (e.g., angled frontal, rear, and side impact) crash configurations.

VISUALIZATION AND MODEL IMPROVEMENT

- Develop impact-condition material property inputs for the foam material used in the current FMVSS 213 test bench. Data to be generated via component-level testing. We believe this will greatly improve correlations of simulations and experiments.
- Incorporate large CRS shell FE mesh in the final model and repeat selected simulations to evaluate mesh-size effects on the fidelity of shell strain prediction and occupant kinematics and injury-indicating parameters.
- At present, the NCVM serves largely as a post-processing utility. In other words, the MADYMO simulation is presented a load case and a set of initial conditions, the analysis simulation executes, and the output files (.kn3, .lac, .fai, etc.) are subsequently generated. As mentioned previously, it is these output files that are then parsed and utilized in the NCVM. The authors envision a more sophisticated simulator wherein the analysis and visualization modules operate in conjunction with one another; the NCVM producing visual imagery "on the fly" as the data is generated by the MADYMO simulation each time step. This will allow the analysis to be performed on one computer in one location, while the visualization proceeds on another computer, in another location, nearly simultaneously. We have already begun to incorporate this functionality into the overall simulation scheme through the use of Parallel

Virtual Machine (PVM) [22, 23]. PVM was chosen as it has proven reliable for message passing on the Windows environment, and also within cross-platform heterogeneous computing environments. This is desirable for the CRS-NCVM research effort as we may have some users on a Workstation (Unix) platform and others on PC (Windows) platforms. A "Master-Slave" model will be utilized; the MADYMO simulation (Master) will perform the analysis, and rather than store the iterational data in one massive data file at the end of the simulation, the data will be delivered immediately, in near-real time, to the NCVM (Slave) for visualization. In this way, the NCVM will receive the current data each iteration, and process the most recent analysis/geometry data as it becomes ready. This eliminates the need for massive array storage requirements upfront, which will help to lessen run-time memory resources. Early experiments have shown that message passing latency (between Master/Slave) is on the order of 10^{-4}, and is thus more than acceptable for maintaining a (visually desirable) 60 Hz frame display rate.

ACKNOWLEDGEMENTS

The authors would like to thank David P. Roberts, Facility Manager of General Dynamics' HYGE Sled Facility, and his entire sled test team for conscientiously applying their individual and collective expertise on behalf of this research. The authors would also like to acknowledge the funding support of the Calspan-UB Research Center (CUBRC) and the Center for Transportation Injury Research (CenTIR). Specifically, the authors thank Alan Blatt of General Dynamics and John Lordi of the University at Buffalo for their valuable advice and guidance in this project. Finally, Dr. Hulme would like to acknowledge the partial funding support of the New York State Assembly for their financial support of NYSCEDII, the research organization for which the NCVM portion of the present research work was performed.

REFERENCES

[1] Title 49 CFR: Part 571, Federal Motor Vehicle Safety Standard 213, "Child Restraint Systems."

[2] Department of Transportation Laboratory Test Procedure # TP-2 13-04, September 1, 1997.

[3] "MADYMO Manuals, Version 5.4, Revision 1.4", (web link), TNO Automotive, July, 1999. www.MADYMO.com.

[4] Trinca, G.W., and Arnberg, W., "Evaluation of different types of child restraint systems for cars." Accident Analysis & Prevention, Volume 13, Issue 1, March 1981, Pages 11-16.

[5] Rudin-Brown, C.M., Kumagai, J.K., et al., "Usability issues concerning child restraint system harness design." Accident Analysis & Prevention, Volume 35, Issue 3, May 2003, Pages 341-348.

[6] Lefeuve, J., Verron, E., et al., "Numeric simulation of a child restraint seat, Mécanique & Industries." Volume 3, Issue 2, 2002, Pages 201-208.

[7] Arbogast, K., Durbin, D. et al., "An evaluation of the effectiveness of forward facing child restraint systems." Accident Analysis & Prevention, In Press, June, 2003.

[8] Carlsson, G. and Ysander, H.N., "Rearward-facing child seats—The safest car restraint for children?" Accident Analysis & Prevention, Volume 23, Issues 2-3, April-June 1991, Pages 175-182.

[9] Czernakowski, W. and Müller, M., "Misuse mode and effects analysis—An approach to predict and quantify misuse of child restraint systems." Accident Analysis & Prevention, Volume 25, Issue 3, June 1993, Pages 323-333.

[10] Noureddine, A., Eskandarian, A., and Digges, K., "Computer modeling and validation of a hybrid III dummy for crashworthiness simulation." Mathematical and Computer Modeling, Volume 35, Issues 7-8, April 2002, Pages 885-893.

[11] Arlt, F. and Marach, A., "CAD modeling of a human 3D child body." International Journal of Industrial Ergonomics, Volume 22, Issues 4-5, 1 November 1998, Pages 333-341.

[12] Thacker, J.G., Reagan, S.W., et al., "Experiences during development of a dynamic crash response automobile model." Finite Elements in Analysis and Design, Volume 30, Issue 4, 15 October 1998, Pages 279-295.

[13] Klinich, K.D., Hulbert, G.M., and Schneider, L.W., "Estimating infant head injury criteria and impact response using crash reconstruction and finite element modeling." Stapp Car Crash Journal, Vol. 46, Nov. 2002, p. 165-194. Report No.: SAE 2002-22-0009.

[14] Grant, R.H., Brutel, G., et al., "The investigation of accidents involving restrained children as part of the CREST project (Child Restraint System for Cars)." International IRCOBI Conference on the Biomechanics of Impact, Goteborg, Sweden, September, 1998, pp. 73-87.

[15] Kayvantasch, K., "Advanced Technologies for Virtual Testing – A European Approach." 3rd Annual European Vehicle Passive Safety Network Conference, Brussels, Belgium, October, 2002.

[16] Wismans, J., "Integrated Project on Advanced Protective Systems (APROSYS)." European Vehicle Passive safety Network, 2nd Partner's Meeting, Brussels, Belgium, March, 2003.

[17] Hybrid III 3 year old (revision 1.4 of d3hyb33y.dat), in TNO-MADYMO, "Database Manual, Version 5.4." Delft, The Netherlands, July, 1999.

[18] "Hypermesh v5.0 User's Manual", (web link), Altair Engineering. http://www.altair.com/software/hw_hm.htm.

[19] Technical Report on dynamic crash test series conducted using modified FMVSS 213 test bench assembly, NAWCADPAX/TR2003.

[20] Woo, M., Neider, J., Davis, T., and Shreiner, D., "OpenGL Programming Guide, Third Edition." Addison-Wesley Publishing, Reading, MA, 2000.

[21] Bourke, P., "Creating Anaglyphs Using OpenGL." On-line web reference: http://astronomy.swin.edu.au/~pbourke/opengl/redblue/, August, 2000.

[22] Geist, G.A., Kohl, J.A., and Papadopoulos, P.M., "PVM and MPI: a Comparison of Features." Calculateurs Paralleles Vol. 8 No. 2, June, 1996, pp. 137-150.

[23] Geist, A., Beguelin, A., Dongerra, J., Weicheng, J., Mancheck, R., and Sunderam, V., "PVM: Parallel Virtual Machine - A User's Guide and Tutorial for Networked Parallel Computing." The MIT Press, Cambridge, MA, 1994.

CONTACT

Kevin F. Hulme, Ph.D.
Research Associate
NYSCEDII
5 Norton Hall
University at Buffalo
Buffalo, NY 14260-1810
716-645-2685 x103
hulme@buffalo.edu

Robert A. Galganski
Senior Engineer
Advanced Information Engineering Services
General Dynamics
P.O. Box 400
4455 Genesee Street
Buffalo, NY 14225
716-631-6892
robert.galganski@gd-ais.com

Abani Patra, Ph.D.
Associate Professor
Mechanical and Aerospace Engineering
605 Furnas Hall
University at Buffalo
716-645-2593 x2240
abani@eng.buffalo.edu

Natarju Vusirikala
Research Assistant
Mechanical and Aerospace Engineering
804 Furnas Hall
University at Buffalo
716-645-2593 x2239
nv5@eng.buffalo.edu

Ioannis Hatziprokopiou
Mechanical Engineer
Advanced Information Engineering Services
General Dynamics
P.O. Box 400
4455 Genesee Street
Buffalo, NY 14225
716-632-7500 x5503
ioannis.hatziprokopiou@gd-ais.com

APPENDIX

Test no.	Maximum forward position of dummy[1] (inches)		Maximum CRS displacement[4] (inches)	Maximum chest resultant acceleration[5] (Gs)	Head Injury Criterion in specified time interval[6]	
	Head[2]	*Knee target*[3]			*15 ms*	*36 ms*
11-3-01	21.6	25.2	3.7	38.5	239	409
11-3-02	21.8	23.8	4.3	40.8	272	438
11-3-03	21.7	25.2	4.3	40.7	281	485
Avg. value	21.7	24.7	4.1	40.0	264	444

[1] Measured in the horizontal (x) direction relative to the test bench pivot point, independent of dummy pre-test location.
[2] Most forward part of the head.
[3] Knee target center.
[4] Measured in the x direction relative to its pre-test location.
[5] Three-millisecond (ms) clipped value calculated before CRS impact with test bench seat back during rebound.
[6] Excludes effects of CRS impact with test bench seat back during rebound.

Table 1: Selected dummy and CRS responses measured in tethered-condition sled testing

Test no.	Maximum forward position of dummy[1] (inches)		Maximum CRS displacement[4] (inches)	Maximum chest resultant acceleration[5] (Gs)	Head Injury Criterion in specified time interval[6]	
	Head[2]	*Knee target*[3]			*15 ms*	*36 ms*
11-3-04	20.9	23.7	6.7	37.1	203	373
11-3-05	21.2	23.9	7.0	38.6	229	392
11-3-06	22.0	24.3	6.6	35.9	217	388
Avg. value	21.4	24.0	6.8	37.2	216	384

[1] Measured in the horizontal (x) direction relative to the test bench pivot point, *independent of dummy pre-test location.*
[2] Most forward part of the head.
[3] Knee target center.
[4] Measured in the x direction *relative to its pre-test location*.
[5] Three-millisecond (ms) clipped value calculated before CRS impact with test bench seat back during rebound.
[6] Excludes effects of CRS impact with test bench seat back during rebound.

Table 2: Selected dummy and CRS responses measured in untethered-condition sled testing

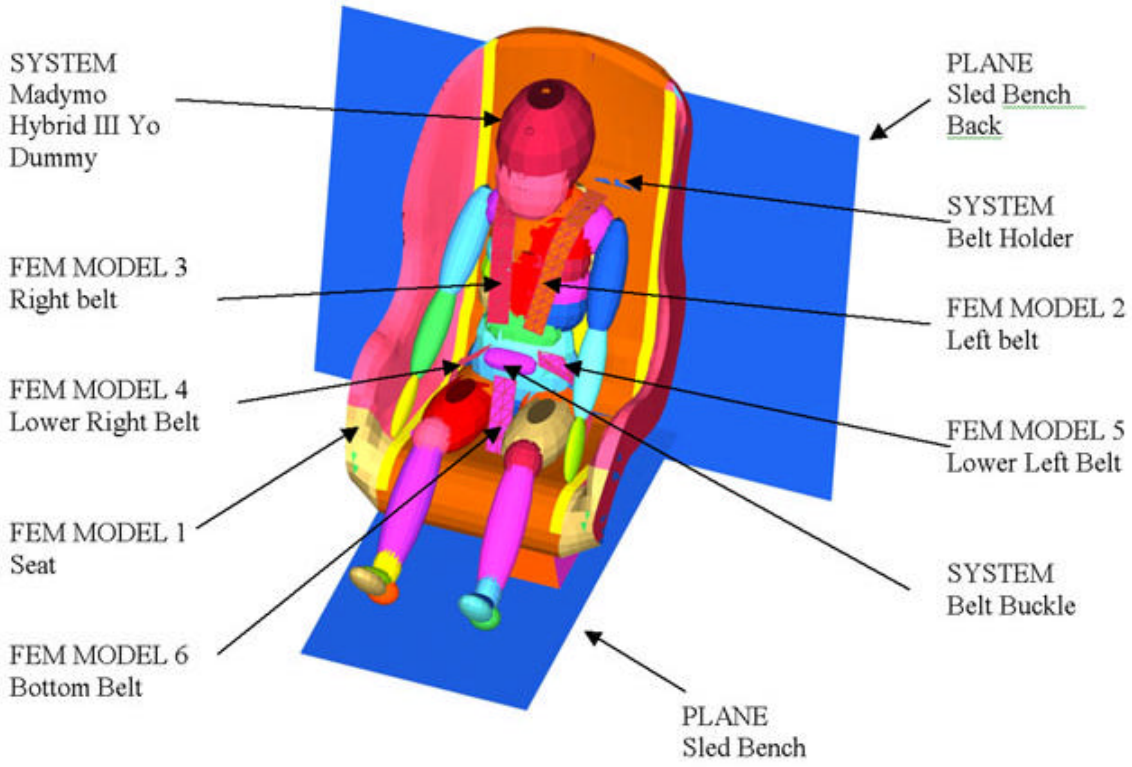

Figure 14: Composite MADYMO CRS model

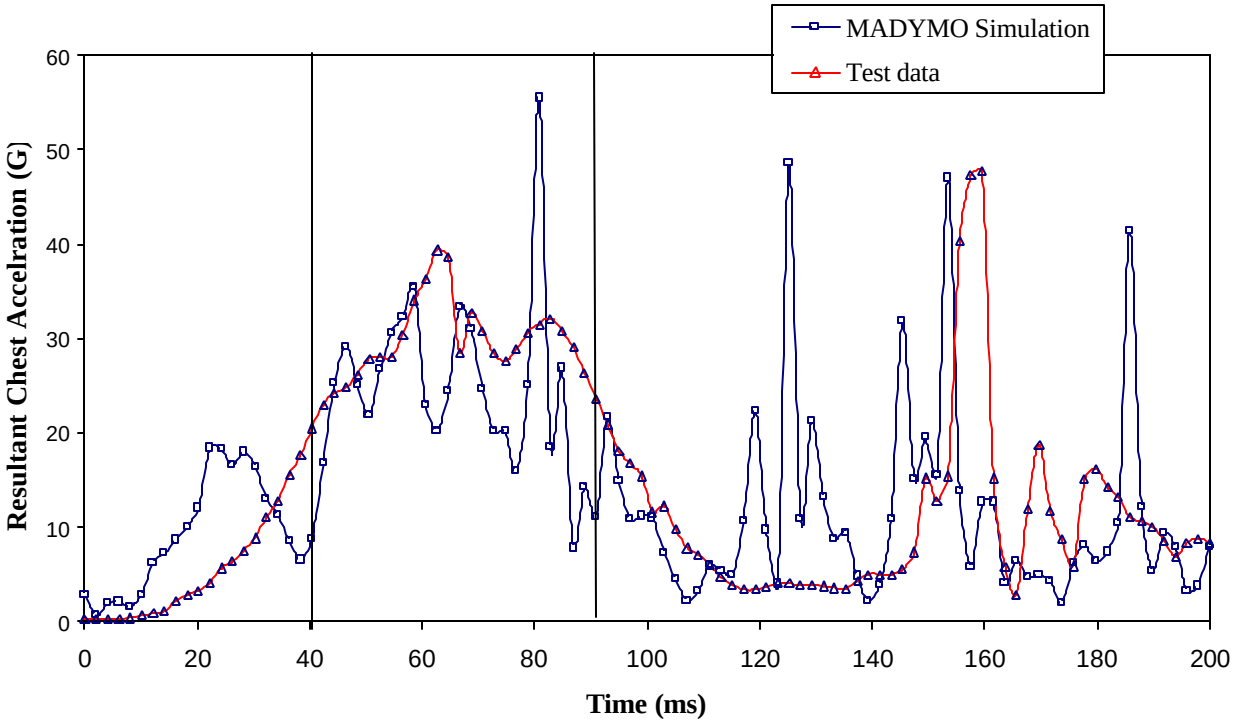

Figure 23a: Resultant Chest acceleration

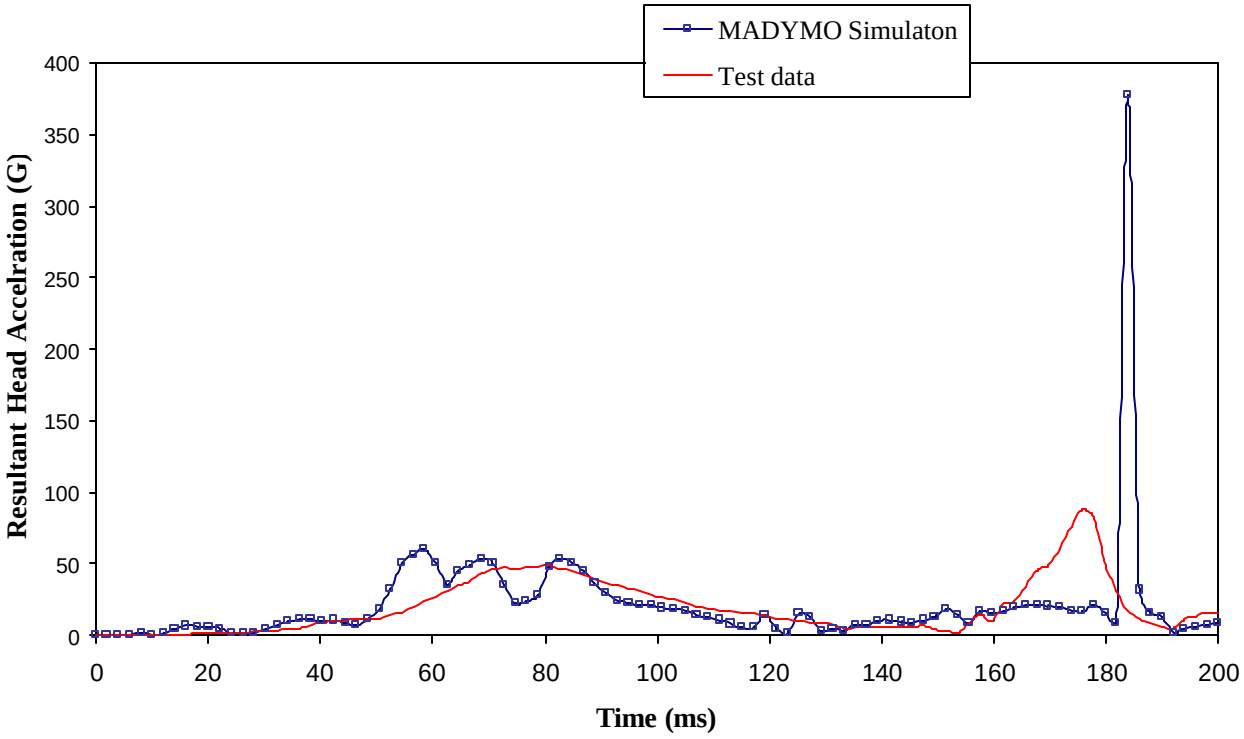

Figure 23b: Resultant Head acceleration

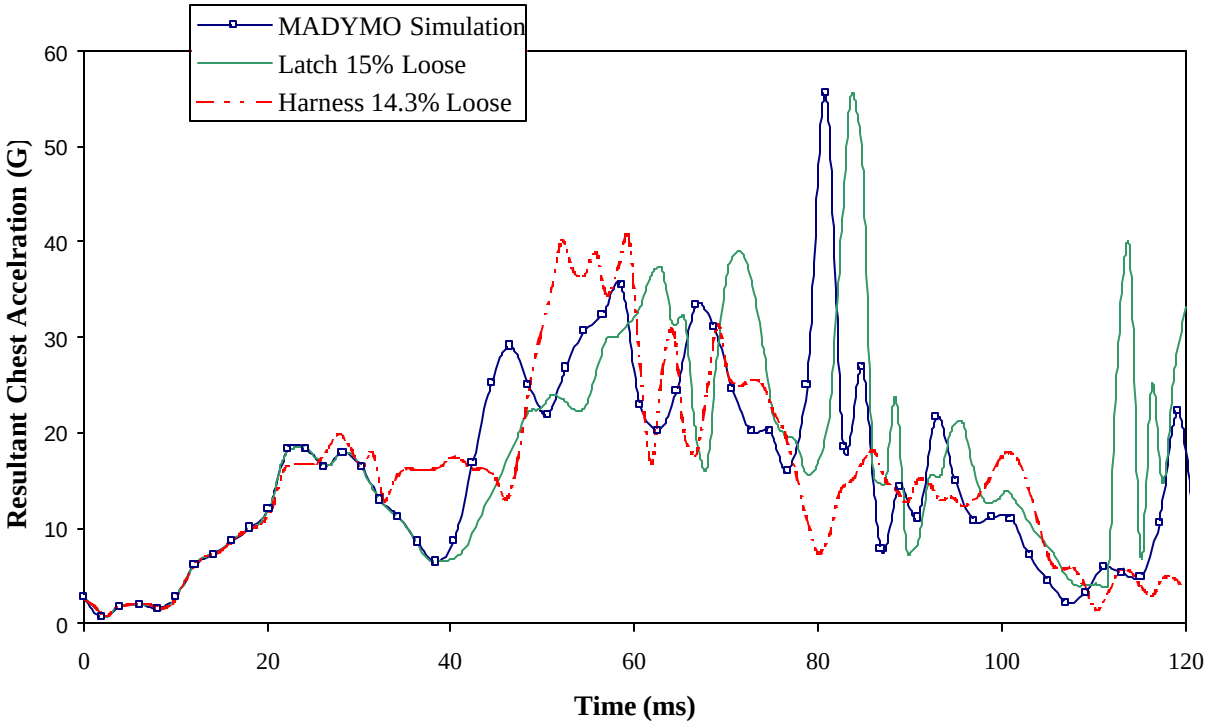

Figure 26: Chest resultant acceleration during misuse